Molecular Dynamics and DFT Studies of Intermolecular Hydrogen Bonds between Bifunctional Heteroazaaromatic Molecules and Hydroxylic Solvents

A. Kyrychenko,† Y. Stepanenko, and J. Waluk*

Institute of Physical Chemistry, Polish Academy of Sciences, Kasprzaka 44, 01-224 Warsaw, Poland

Received: March 9, 2000; In Final Form: June 12, 2000

Molecular dynamics (MD) and ab initio/density functional theory (DFT) studies were performed for alcohol and water complexes of 1H-pyrrolo[3,2-*h*]quinoline (**PQ**), 2-(2′pyridyl)indole (**PyIn-2**), and 7-azaindole (**7AI**). The experiment shows that these molecules form different types of intermolecular complexes with hydroxylic solvents in the ground electronic state. The solvates of **PQ** consist mostly of cyclic, doubly hydrogen-bonded species; in **PyIn-2**, both cyclic and noncyclic forms are detected, while in **7AI** the ground state population of cyclic species seems to be negligible. Our calculations correctly reproduce these observations and allow predictions for water solvates that have not been yet studied experimentally. MD simulations show that for **PQ,** the population of cyclic 1:1 species is dominant even in bulk methanol. On the contrary, no such species are predicted in bulk methanol for **7AI**. Three forms are obtained for **PyIn-2** in bulk methanol: one cyclic and two noncyclic ones, with comparable populations. Simulations of dilute mixtures with methanol in *n*-hexane reveal that a 1:1 cyclic structure is preferable in all compounds. At 1:2 stoichiometry, differences arise between **PQ** and **PyIn-2**, which still form mainly cyclic 1:1 complexes solvated by another alcohol molecule, and **7AI**, which preferentially forms a triply hydrogen-bonded, quasi-eight-membered ring structure. These differences are retained in bulk methanol. DFT results predict that the stability of the cyclic 1:1 complexes with methanol increases in the order **7AI** < **PyIn-2** < **PQ**. An opposite trend is obtained for 1:2 solvates that form a closed network of three hydrogen bonds.

1. Introduction

Influence of hydrogen bond formation upon photophysical characteristics has been a subject of intense investigation of a large variety of heteroazaaromatic molecules.[1−57] It has been shown that intermolecular hydrogen-bonding may alter completely the excited-state behavior of a chromophore. It also plays a crucial role in many photochemical and photobiological processes. Among various hydrogen-bonded systems studied, a particular class of azaaromatic compounds—those mimicking the behavior of nucleic base pairs—has attracted considerable interest. A classical example of such system is provided by 7-azaindole (**7AI**).[5−43] The photophysics of **7AI** continues to be a subject of extensive studies and controversies since the discovery of the excited-state double proton transfer (ESDPT) in the **7AI** dimer.[5] Recent developments of femtosecond spectroscopy, supersonic jets, and mass spectroscopy detection enabled a detailed study of this process, both in the gas phase[6−8] and in solution.[9−11] It has also been recognized that the ESDPT process can occur in bulk protic solvents, assisted by formation of a cyclic, doubly hydrogen-bonded complex between **7AI** and one hydroxylic solvent molecule. The photophysics of chromophores related to **7AI** (for example, 1-azacarbazole (**1AC**)),[44−47] is still attracting considerable attention, as it has a great potential for probing the solvation dynamics and modeling the radiation-induced processes in DNA base pairs.

* Author to whom correspondence should be addressed. Prof. Dr. Jacek Waluk, Institute of Physical Chemistry, Polish Academy of Sciences, Kasprzaka 44/52, 01-224 Warsaw, Poland. Fax: (+48) 391 20 238. E-mail: waluk@ichf.edu.pl.

† Permanent address: Research Institute for Chemistry, Kharkov State University, 4, Svobody Sq., 310077 Kharkov, Ukraine. Present address: Department of Physical Chemistry, Chalmers University of Technology, SE-412 96 Gothenburg, Sweden.

CHART 1: Two-step Mechanism of ESDPT in 7AI:Alcohol Complexes

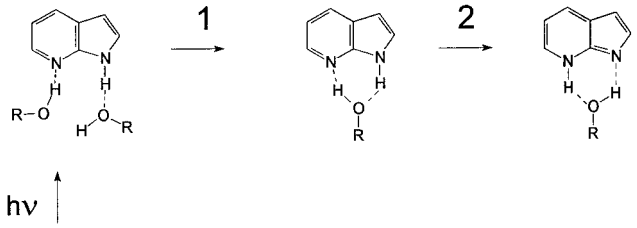

Several groups studied the ESDPT phenomenon in **7AI** alcohol and water solutions.[12−24] A two-step mechanism has been proposed, involving, first, the excited-state solvent rearrangement toward a favorable structure, and, second, the actual proton transfer (Chart 1). It has been suggested that **7AI** molecules in a bulk alcohol solvent exist in a wide range of hydrogen-bonded structures. Only a selected part of the equilibrium population possesses an appropriately hydrogen-bonded structure, able to phototautomerize directly and rapidly, just as in the case of the dimer. The activation energy of the tautomerization has been found to correlate with the activation energy of viscous flow in alcohols,[18] implying that the rate-controlling step should involve large-amplitude solvent motions around an excited **7AI** molecule in order to enable the ESDPT in alcohols. Hence, it was concluded that solvent rearrangement toward an appropriate configuration is required prior to the fast double proton-transfer event.[16,17] On the other hand, it was also postulated that the proton-transfer itself may be the rate-limiting step of the overall kinetics.[21] It may also be that none of these steps is completely rate-determining. Despite the controversies regarding the rate-controlling step of the mechanism, it is

10.1021/jp000921w CCC: $19.00
Published on Web 09/29/2000

generally agreed that the structure of the precursor for the ESDPT corresponds to a 1:1 cyclic double hydrogen-bonded complex with an alcohol molecule. Both experimental and theoretical studies indicate that in **7AI** such structure is formed after excitation. Thus, ESDPT occurs after solvent rearrangement around an excited solvate. The fraction of complexes "prepared" for tautomerization already in the ground state is very low, probably below 1%.[41]

Initial studies of the photophysics of **7AI** in water gave no indication of an ESDPT reaction. However, detailed examination of the fluorescence kinetics in bulk water revealed a spectral inhomogeneity of the emission band and showed double exponential fluorescence decays and growths. Two completely different explanations were proposed. According to the first one, phototautomerization in water is qualitatively the same as in alcohols.[19] The process takes about 900 ps, much longer than in alcohol solutions. In the other model, it is argued that in water only a small fraction of **7AI** complexes can undergo a rapid (70 ps) tautomerization, and that the structure of the solvates is dominated by "blocked" species, for which the time required for solvent rearrangement leading to the tautomer is estimated to be longer than 10 ns.[22] Also for alcohol solvents, it was postulated that a fraction of "blocked" complexes exists.[20]

The detailed structure of the precursor and the ESDPT mechanism are extremely difficult to determine in bulk water or alcohols. To minimize the effects of solvent self-aggregation on ESDPT in bulk water, some authors have examined the dilution of water in aprotic solvents. Nice confirmation of the occurrence of ESDPT in water was provided by experiments in which the tautomeric fluorescence could be induced by saturating ethyl ether or *p*-dioxane solutions with water.[23] It was concluded that the **7AI** monohydrate, formed under such conditions, can undergo phototautomerization, and that the reaction is not possible for polyhydrates, prevalent in bulk water. Similar results have been obtained for **1AC** upon addition of small amounts of alcohol to *n*-hexane or cyclohexane solutions.[46] It has been shown that, in such dilute mixed solutions, the dominant species correspond to 1:1 cyclic hydrogen-bonded **1AC**/solvent complexes, able to undergo ESDPT. An important observation was that the proton-transfer emission, produced under such conditions, becomes less intense with the increasing content of protic components in the mixture. It has been postulated that this finding reflects the partial disappearance of the cyclic complexes and the gradual formation of different solvates with noncyclic hydrogen-bonding. The latter are unable to tautomerize, due to participation in a network of hydrogen-bonds.

Dilute solution studies made it possible to clarify some questions concerning the structure of a precursor of the ESDPT process. However, the most detailed characteristics of such complexation could be extracted from supersonic jet experiments. A large variety of jet-cooled **7AI**[32−35] and **1AC**[47] clusters were studied. The analysis of rotationally resolved laser-induced fluorescence (LIF) spectra of jet-cooled **7AI-(H$_2$O)$_n$** clusters with *n* up to 3 has allowed the authors to propose that the structure of the **7AI-H$_2$O** solvate corresponds to a cyclically hydrogen-bonded complex.[32] The **7AI-(H$_2$O)$_2$** and **7AI-(H$_2$O)$_3$** clusters are also expected to be arranged in the planar ring backbone, forming a closed network of hydrogen-bonds with eight- and ten-membered rings, respectively. On the other hand, other authors claim that **7AI-H$_2$O** and **7AI-MeOH** clusters do not necessarily correspond to a cyclic hydrogen-bonded geometry because the estimated stability of these structures would not correlate with the size of the red shift in the LIF spectrum.[34]

CHART 2: Bifunctional Molecules Which undergo ESDPT in Hydrogen-Bonded Complexes with Alcohols

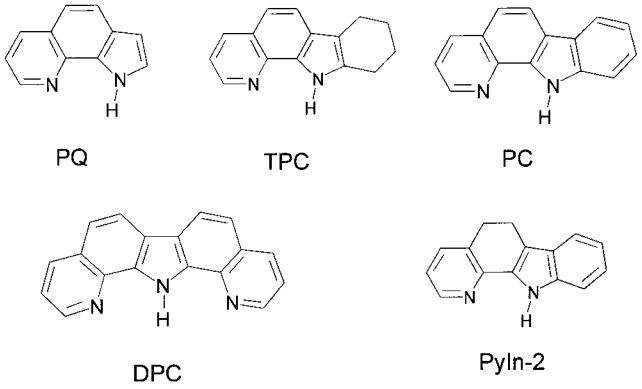

Several ab initio and molecular dynamics (MD) studies have been performed to clarify the structure and different stability of cyclically hydrogen-bonded complexes of **7AI** with various molecules.[25−27,36−43] It has been shown that a change in the local topology of hydrogen-bonding sites of a solvent molecule (for example, substituting methanol or water by acetic acid) can cause an additional exothermicity of complexation due to formation of a cyclic complex with more favorable geometry, in which both distances and the angles of the doubly hydrogen-bonded ring can be adjusted more freely.[26] However, to deeply understand the mechanism of a specific solvation at a molecular level it is necessary to take into account the total solvent effect. Recent works by Maroncelli's group have examined the behavior of **7AI** and **1AC** in dilute mixed solutions as well as in bulklike protic solvents by means of Monte Carlo and MD simulations.[41,42] The authors have shown that the cyclic complexation is the predominant solvation mode of **7AI** in a dilute solvent mixture. On the contrary, in bulklike hydroxylic environment the two hydrogen-bonding sites are involved in separate hydrogen-bondings with solvent molecules.

Recently, a new family of bifunctional heteroazaaromatic compounds has been investigated. Similarly to **7AI**, these molecules possess both, a hydrogen-bond donor (an aromatic NH group) and an acceptor (a pyridine-type nitrogen atom).[48−57] The series included 1H-pyrrolo[3,2-*h*]quinoline (**PQ**), 7,8,9,-10-tetrahydropyrido-[2,3-*a*]carbazole (**TPC**), pyrido[2,3-*a*]carbazole (**PC**), dipyrido[2,3-*a*:3′,2′-*i*]carbazole (**DPC**), and 2-(2′pyridyl)indole (**PyIn-2**) (Chart 2). In alcohol solutions, an ESDPT reaction was observed for all these molecules, manifested by dual fluorescence. It was shown that the proton transfer occurs in a 1:1 cyclic doubly hydrogen-bonded complex of an excited chromophore with an alcohol molecule. The photoreaction rates are extremely fast. Two components, 600−900 fs and 6−11 ps, were observed at room-temperature both in the decay of the primary fluorescence and in the rise of tautomeric emission.[50] Most important, the cyclic precursor for the ESDPT reaction is formed *already on the ground-state level*. The excited-state behavior of the species that originally are not arranged in a cyclic complex differs from that of structurally related chromophores of **7AI** and **1AC**. In our compounds, the excited noncyclic solvates undergo a not-ESDPT type of radiationless $S_1 \rightarrow S_0$ depopulation. This process is strongly dependent on temperature and solvent viscosity. An intriguing finding was that the relative population of the cyclic ground-state complexes varies strongly across the series. For **DPC**, **PQ,** and **TPC,** the cyclic species dominate even in bulk alcohols and at low temperatures, while for **PC** and **PyIn-2** this is not the case. In the former three molecules, the ground-state population of cyclic complexes is

about 2 orders of magnitude higher that in the case of **7AI**. **PyIn-2**, in turn, represents an intermediate case, with the population of cyclic species lower than in **DPC**, **PQ**, and **TPC**, but still much higher than in **7AI**. The experimental accuracy (±50% in worst cases) does not allow a very precise determination of the fractions of cyclic and noncyclic species, but it is safe to estimate that while the cyclic complexes comprise about 50% in **PQ**, their fraction is definitely smaller in **PyIn-2**.

The purpose of the present work is to find whether the experimentally observed differences between **7AI** and our bifunctional molecules can be rationalized by theoretical calculations. The main goal was to account, on one hand, for structural variations in hydrogen-bonded solvates of **7AI** and our molecules and, on the other hand, for quantitative differences within the series. Preliminary results suggested that molecular dynamics, in particular, may be helpful in predicting the ratio of cyclic to noncyclic species in bulk methanol.[48] The specific issues addressed in this work regard the following: (i) the structure of 1:1 complexes with methanol and water; (ii) structure and stability of higher-order complexes; (iii) relative populations of different types of solvates in bulk methanol and water; (iv) comparison of solvate structures in dilute and bulk methanol and water solutions for each molecule under investigation; (v) differences between the three molecules observed for the same solvent; (vi) differences between water and alcohol complexes.

Molecular dynamics and DFT calculations were performed for **7AI**, **PQ,** and **PyIn-2** in their ground electronic states. Molecular dynamic simulations were done first for diluted nonpolar solutions containing methanol and water solvates of 1:*n* stoichiometry, with $n = 1,2$ and, for some cases $n = 3,4,5$. Next, calculations were performed for bulk methanol and water solutions. The results of molecular dynamics simulations were compared with structural and energy data obtained by DFT calculations for 1:1 and 1:2 complexes.

Molecular dynamics simulations fare surprisingly well, both when predicting properties of a given chromophore in different environments and when comparing different molecules in the same type of solvent. The results of DFT studies are in agreement with the experimental data regarding relative stabilities of various types of complexes in bulk protic solvents. However, in the case of DFT calculations, quantitative predictions concerning, for instance, fractions of different forms, are rather difficult to make.

2. Computational Details

All ab initio calculations were performed using the Gaussian 98 suite of programs.[58] Ground-state geometries and energies of individual molecules and complexes were obtained at the B3LYP/6-31G(d,p) level. Optimized structures were verified to correspond to the minima by calculating and diagonalizing the matrix of the second derivatives of energy (Hessian) and establishing that there are no negative eigenvalues. The energy of complex formation was then computed as the difference between the energy of the pair and the energies of individually optimized complex partners, including the zero-point vibration energy (ZPE) correction. Next, basis-set superposition error (BSSE) correction was introduced, obtained using the counterpoise technique. The absolute values of BSSE are quite large, about 4 kcal/mol for 1:1 complexes and 50% higher for 1:2 solvates. Therefore, a comparison of calculated hydrogen-bonding energies for a given type of complex can be considered meaningful only when the BSSE values are not structure-dependent. Fortunately, this was found to be the case. The values

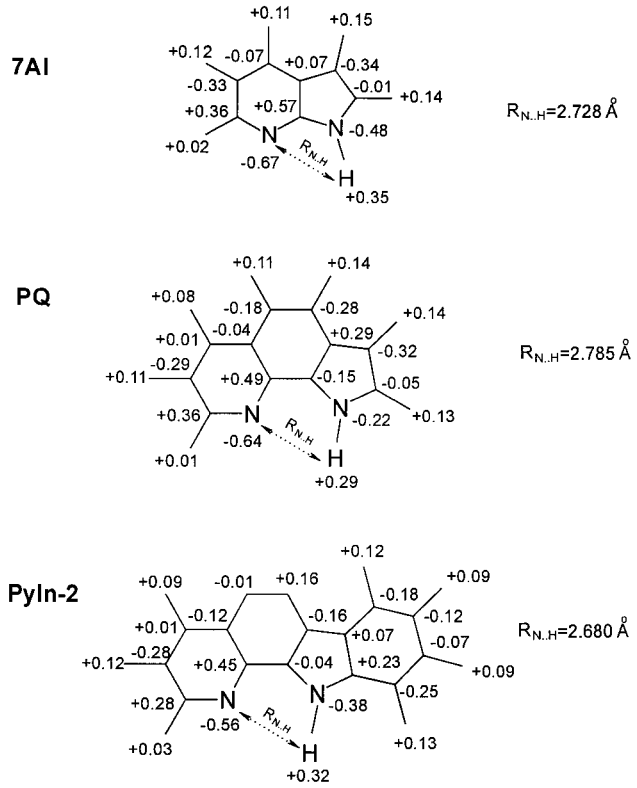

Figure 1. The charges on **7AI**, **PQ,** and **PyIn-2** used in MD simulations, generated by electrostatic potential fits of the ground-state B3LYP wave functions obtained using a 6-31+G(d,p) basis set.

of BSSE calculated for each of the three molecules turned out to be practically the same (within ±0.2 and ±0.5 kcal/mol for 1:1 and 1:2 solvates, respectively) for each type of complex. The MOLDEN package[59] has been used for the presentation of results.

Molecular dynamics studies were performed with the GROMOS96 package of programs[60] with the 43A1 force field.[61] A mixed representation, ab initio combined with the 43A1 force field, was used for modeling the solute. A rigid all-atom model was used for the solute molecule. GROMOS96 force field parameters corresponding to bond lengths and angles were adjusted in order to retain the B3LYP/6-31+G(d,p) level optimized geometry of the solute. For **PyIn-2**, internal rotation around a single C−C bond connecting the pyridine and pyrrole moieties was modeled by a torsion potential of an aliphatic CH_2-CH_2 bridge. Thus, in this molecule, restricted motion was allowed about the bond joining the two parts. Multiple-center point charge distribution was used with each solute atom treated as a separate charge group. Partial charges needed for Coulomb interactions were derived for the B3LYP/6-31+G(d,p) optimized geometry using the ChelpG procedure implemented in the Gaussian 98 program. The optimized atom-centered point charges derived by this method produce, in our opinion, the best least-squares fitting to the molecular electrostatic potential surface calculated using the molecular wave function. Figure 1 presents the ESP charges that were used in MD simulations. The standard van der Waals parameters were taken from the GROMOS96 force field without changes. Common van der Waals parameters for pyridine and pyrrole nitrogen atoms were used for modeling of hydrogen-bonding in all three solutes under study. The aliphatic hydrogen atoms of a solvent were treated as united atoms together with the carbon atom to which they are attached. All force field parameters for methanol and SPC/E-water models were taken from the GROMOS96 solvent

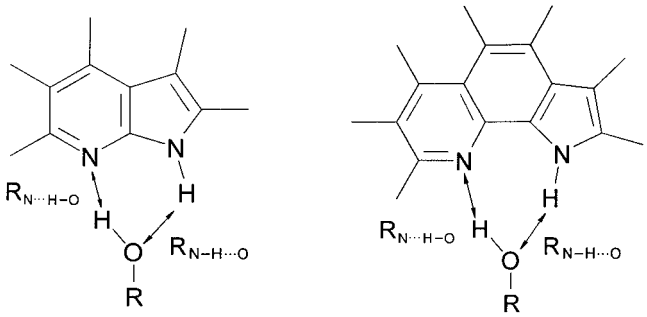

Figure 2. The definition of $R_{N-H\cdots O}$ and $R_{N\cdots H-O}$.

library.[61] For *n*-hexane, the force field parameters were adapted from ref 62 and were close to those of the GROMOS96 parametrization for the aliphatic CH_n united atoms.[61] Internal rotations around $-CH_2-CH_2-$ dihedral angles were modeled using a standard GROMOS96 torsion potential energy function for these groups. The standard pairwise additive effective potential[61] E_{ab} of the van der Waals plus Coulomb (electrostatic) form was used to represent nonbonded interactions between sites *i* and *j*.

The solute molecule was placed in the center of a rectangular box, filled with solvent at an equilibrium distribution. Solvent molecules lying outside the box or overlapping with solute atoms (solute−solvent distance < 2.3 Å) were removed. The final systems included 116 and 216 solvent molecules for *n*-hexane, and methanol or water, respectively. For each system, the energy minimization was first performed to obtain the starting structure for molecular dynamic simulations. Initial velocities in the starting ensemble were taken from a Maxwell distribution at 250 K. This was followed by a 50 ps simulation of solvent equilibration at constant temperature and volume, and by another 50 ps at constant temperature and pressure. The whole system was then allowed to relax for 100 ps, after which the trajectories, saved every 10 fs, were being collected for 500 ps. All simulations were performed using periodic boundary conditions at temperature of 300 K and pressure of 1 atm. The temperature and pressure were maintained by weak coupling to an external bath,[63] using a relaxation time of 0.1 and 0.5 ps, respectively. The bond lengths were constrained using the SHAKE algorithm[64] with geometry tolerance of 10^{-4}. The integration time step was 0.5 fs. A cutoff radius of 1.1 nm in the case of methanol and water, and 1.4 nm in the case of *n*-hexane, was used for nonbonded interactions, which were calculated at each time step using a charge-group pair list that was updated every 20 time steps. The results of MD simulations were visualized by the gOpenMol program.[65]

3. Results and Discussion

Using classical MD simulations, we have explored various solvation structures of **PQ** and **PyIn-2**. The simulations for **7AI** have been repeated in order to test the agreement between the results obtained by our MD approach and those obtained previously by other authors.[41] Bifunctional molecules—**7AI**, **PQ** and **PyIn-2**—possess two centers able to form hydrogen-bondings with the solvent. The hydrogen-bond between the pyridine-type nitrogen atom and the solvent hydroxylic hydrogen is labeled "N···H−O", while that between the hydrogen atom of the pyrrole NH group and the solvent oxygen atom is referred to as "N−H···O". The two hydrogen-bond distances are presented in Figure 2 for **7AI** and **PQ**. The same designations are used for **7AI, PQ**, and **PyIn-2**. The intermolecular hydrogen-bonding between a bifunctional solute and a solvent is analyzed in terms of the hydrogen-bonding distance distribution (HBD distribution), which displays a relative frequency of a simultaneous occurrence of a pair of $R_{N-H\cdots O}$ and $R_{N\cdots H-O}$ distances within an hydrogen-bonded complex. Such 3D presentation of an hydrogen-bonding distribution has recently been shown to be quite useful.[41] Both $R_{N-H\cdots O}$ and $R_{N\cdots H-O}$ distances between the solute "active sites" and the "H" and "O" centers of each solvent molecule have been calculated at every MD step along a coordinate trajectory file, but the corresponding hydrogen-bond values have been added to an HBD distribution only when both hydrogen-bond distances had been simultaneously found to be smaller than the cutoff distance equal to 7 Å.

Figure 3 presents the HBD distributions for 1:1 complexes of **7AI**, **PQ,** and **PyIn-2** with one methanol molecule in *n*-hexane solution. The most probable values for a pair of distances of both hydrogen-bonds in the HBD distribution span a range from 1.9 Å to about 2.5 Å. The population of hydrogen-bonded species, which may be described by such a kind of hydrogen-bonding, corresponds to a complex in which, most of the time, a single methanol molecule is simultaneously hydrogen-bonded to both of the solute "active sites". The structure of such solvate conforms to a cyclic doubly hydrogen-bonded complex between the bifunctional solute and one methanol molecule. In respect to the ability to form the cyclic hydrogen-bonded complexes all molecules under study seem to be similar. However, a closer inspection of Figure 3 shows that, in case of **PQ**, the cyclic doubly hydrogen-bonded complex with one methanol is more "rigid" than the analogous cyclic structure of **7AI**. These differences are revealed by the values of the full width at half-maximum (fwhm) of the HBD distribution peak. For the **PQ-(MeOH)$_1$** complex, the fwhm values along the directions of both hydrogen-bonds are much smaller than in the case of **7AI-(MeOH)$_1$** (Table 1). In the latter case, the HBD distribution shows the occurrence of a fraction of the hydrogen-bonded species with one of the distances exceeding the maximum value for the generally accepted range of hydrogen-bonding, approximately 2.5 Å. Consequently, in such a cyclic solvate, one of the two hydrogen-bonds, N···H−O, occasionally becomes broken. We have estimated the relative equilibrium population of the cyclic complexes versus the noncyclic ones by the following procedure: the HBD distribution of the $R_{N-H\cdots O}$ and $R_{N\cdots H-O}$ values, spanning the range from 0 to 4 Å, was integrated first. The result corresponds to a total integral intensity of the hydrogen-bonding in the first solvation shell around the solute "active sites". Next, the integration was repeated only for the $R_{N-H\cdots O}$ and $R_{N\cdots H-O}$ distances simultaneously smaller than one of two reference cutoffs for hydrogen-bonding, 2.5 Å and 2.2 Å, respectively. The values of these integrals have been used for the definition of the relative equilibrium fractions of the cyclic complexes. Such a procedure yielded the values of 37% and 13% as the fraction of cyclic complexes for **7AI-(MeOH)$_1$** (Table 1). Thus, only for about 13−37% of the time, **7AI** is solvated in a "cyclic manner". In the case of **7AI-(MeOH)$_1$**, the hydrogen-bonding distance between the pyridine-type nitrogen atom and the hydroxylic hydrogen of the methanol molecule exhibits a broad distribution along the N···H−O coordinate, up to 4 Å. Simultaneously, the hydrogen-bonding distances between the pyrrolic hydrogen of **7AI** and the oxygen atom of the methanol span quite a short range, with the fwhm value equal to 0.36 Å. The structure of such hydrogen-bonded species corresponds to a noncyclic, separately hydrogen-bonded complex. In such a noncylic complex, the methanol molecule is preferably hydrogen-bonded mainly to the pyrrolic hydrogen atom of **7AI**. Thus,

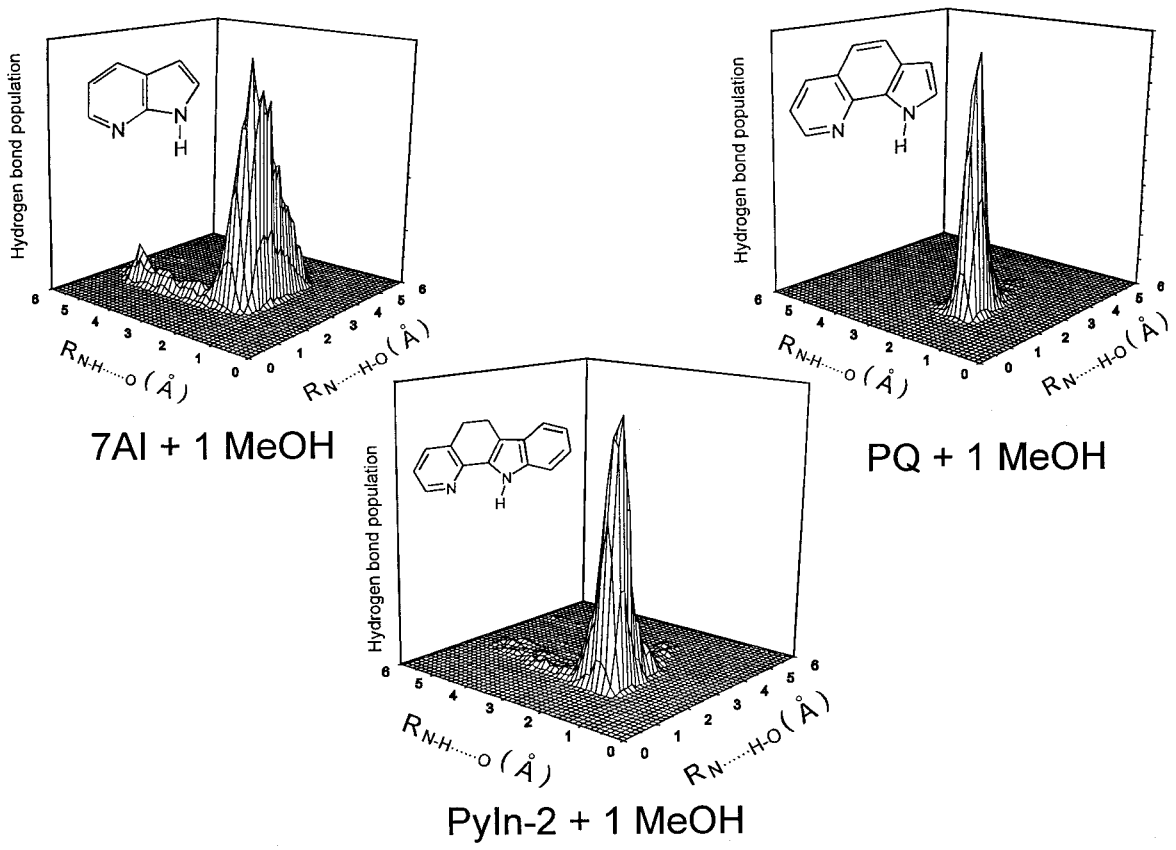

Figure 3. The results of MD simulations for **7AI**, **PQ**, and **PyIn-2** in *n*-hexane containing one molecule of methanol.

the N···H−O bond is broken more frequently than the N−H···O bond. The peak of the **7AI**-(**MeOH**)$_1$ HBD distribution corresponds to a smaller value of the N−H···O than the N−H···O distance. In other words, the average distance of the hydrogen-bonding to the pyrrolic hydrogen is shorter than to the pyridine nitrogen and thus, the two hydrogen-bonds within the cyclic **7AI**-(**MeOH**)$_1$ complex are nonequivalent (Table 1). Mente and Maroncelli have reported similar results using Monte Carlo simulations for **7AI**-**(MeOH)$_1$** complex and also pointed to a stronger hydrogen-bond with the pyrrolic hydrogen.[41] For our study, more important is that, under the same conditions as for **7AI**, **PQ** forms the most "rigid" doubly hydrogen-bonded complex with quite short average lengths of both hydrogen-bonds. In the case of **PQ**, the cyclic complex was found to persist for 69% and 88% of the time for the two cutoff criteria, respectively. In terms of the structural rigidity, the cyclic, doubly hydrogen-bonded **PyIn-2-(MeOH)$_1$** complex can be regarded as an intermediate between **7AI** and **PQ** solvates. For **PyIn-2-(MeOH)$_1$**, the equilibrium populations of the cyclic species are 50% and 72%.

Addition of a second methanol molecule, leading to **7AI-(MeOH)$_2$** changes the hydrogen-bonding structure within the solvate dramatically (Figure 4). In the HBD distribution, the peak corresponding to the cyclic complex has disappeared and two new peaks have appeared, shifted toward a long-distance region. This new solvation structure conforms to the complex in which each methanol molecule is strongly hydrogen-bonded to only one of the two possible solute "active sites"; simultaneously, the two methanol molecules are hydrogen-bonded to each other. As a result, triply hydrogen-bonded "eight-membered ring" complex is observed. Thus, in the case of **7AI**, a cyclic hydrogen-bonded complex becomes unfavorable when more than one methanol molecule is available. The fraction of cyclic 1:1 species decreases below 1%. A completely different picture is obtained for **PQ-(MeOH)$_2$** solvates. The distribution peak corresponding to the population of the cyclic complex remains at the same position as for **PQ-(MeOH)$_1$**. The average distances of both hydrogen-bonds calculated from the main peak of the **PQ-(MeOH)$_2$** HBD distribution also remain unchanged with respect to the case of **PQ-(MeOH)$_1$** (Table 1). The fwhm value of the main peak along the N−H···O distance is also the same. These findings show that in case of the **PQ-(MeOH)$_2$** solvate, approximately 26−39% of the hydrogen-bonded species still correspond to the 1:1, cyclic, doubly hydrogen-bonded complex. However, the results also show that the addition of the second methanol molecule leads to the appearance of a small population of hydrogen-bonded complexes with a noncyclic structure. The hydrogen-bonding distribution along the N···H−O distance becomes broader and the increase of the corresponding fwhm value (Table 1) can be explained by the presence of another peak located under the main peak of the distribution. The shoulder on the main peak is located at about 3 Å along the N···H−O direction; the corresponding N−H···O coordinate is about 1.8 Å. This shoulder can be attributed to the noncyclic hydrogen-bonded species due to the hydrogen-bonding with the pyrrolic hydrogen of **PQ**. Figure 4 also shows that, upon addition of the second methanol molecule, a small broad peak appears, located at 3.58 Å along the N−H···O coordinate (Table 1). The corresponding N···H−O coordinate is equal to 2.02 Å with the fwhm value of 0.44 Å. The structure of such hydrogen-bonded species conforms to a strongly hydrogen-bonded complex between the pyridine-type nitrogen atom of **PQ** and the hydroxylic hydrogen atom of methanol. Thus, from the HBD distribution presented in Figure 4, at least three different hydrogen-bonded complexes of **PQ** with two molecules of methanol can be revealed: one cyclic and two noncyclic, separately hydrogen-bonded complexes. In the two latter cases, **PQ** is hydrogen-bonded through only one of its two "active

TABLE 1: MD Results: The Maxima of Main Peaks in the HBD Distributions and the Corresponding fwhm Values; The Equilibrium Fractions (in percent) of the 1:1 Cyclic Doubly Hydrogen-Bonded Complex (see text for details)

	peak maximum [Å][a]		fwhm [Å]		equilibrium fraction cutoff [Å]	
	N···H−O	N−H···O	N···H−O	N−H···O	2.5	2.2
PQ + 1 MeOH	2.02	1.76	0.48	0.26	88	69
PQ + 2 MeOH	2.02	1.76	1.00	0.26	39	26
	2.02	3.58	0.44	0.54		
PQ in bulk MeOH	2.02	1.76	1.00	0.26	35	24
	2.15	4.49	0.56	1.22		
PQ + 1 H_2O	1.89	1.89	0.44	0.34	89	70
PQ + 2 H_2O	2.02	1.89	1.00	0.40	42	26
	2.15	3.71	0.52	0.54		
PQ in bulk H_2O	2.02	4.10	0.66	1.30	10	5
	3.19	2.02	1.10	0.40		
PyIn-2 + 1 MeOH	2.02	1.89	0.50	0.42	72	50
PyIn-2 + 2 MeOH	2.15	3.71	0.54	0.52	26	15
	2.54	1.89	1.02	0.30		
PyIn-2 in bulk MeOH	2.15 (a)[b]	1.76	0.58	0.36	15	9
	2.02 (b)	3.45	0.60	0.90		
	3.06 (c)	1.89	0.80	0.34		
PyIn-2 + 1 H_2O	1.89	2.02	0.58	0.36	74	47
PyIn-2 + 2 H_2O	1.89	2.02	0.44	0.40	31	19
	2.02	3.32	0.42	0.70		
PyIn-2 in bulk H_2O	2.15	1.89	0.52	0.32	5	3
	2.02	3.84	0.52	1.10		
	3.32	2.02	0.86	0.56		
7AI + 1 MeOH	2.28	1.89	1.28	0.36	37	13
7AI + 2 MeOH	1.89	3.45	0.34	0.50	1	0.1
	3.19	1.89	0.56	0.24		
7AI in bulk MeOH	1.89	5.14	0.30	0.86	0.9	0.1
	3.84	1.76	0.92	0.26		
7AI + 1 H_2O	2.15	2.15	0.60	0.68	35	11
7AI + 2 H_2O	1.89	3.45	0.26	0.46	0.1	0.01
	3.19	1.89	0.48	0.28		
7AI in bulk H_2O	1.89	4.49	0.30	1.00	0.01	
	3.97	1.89	0.98	0.34		

[a] Accuracy: ± 0.07 Å. [b] Compare with Figure 5.

sites". The relative fractions of both noncyclic complexes were estimated to be approximately equal. It should be noted that such a kind of 3D presentation as used here corresponds to a "static" view of the results of MD simulations. The dynamic behavior within an hydrogen-bonded solvate cannot be clearly traced through the presentation by means of the HBD distribution.

In the case of **PQ-(MeOH)$_2$** solvate, a possibility arises of a competing hydrogen-bonding interaction between the added methanol and the solute, already involved in the cyclic hydrogen-bonded complex with the first methanol molecule. On the other hand, methano−methanol hydrogen-bonding is also possible. The hydrogen-bonding dynamics within the **PQ-(MeOH)**$_2$ solvate could be traced by analyzing the MD trajectories. The general conclusion is that the competition between the two molecules of methanol results in the loss of the rigidity of the 1:1 cyclic hydrogen-bonded complex. Most of the time, the 1:1 cyclic complex was found, with one methanol molecule interacting with the other, already included in the cyclic complex with the solute. As a result, the cyclic hydrogen-bonded structure could be thermally distorted more easily. It is instructive, in this context, to compare the behavior of 1:1 and 1:2 alcohol solvates of **PQ**. For thermal fluctuations causing a structural distortion of the cyclic **PQ-(MeOH)$_1$** complex, a fast relaxation backward to the optimal cyclic structure usually takes place. However, if the analogous distortion is arising in **PQ-(MeOH)**$_2$, the solvate is trying to achieve the optimal structure, but, at the same moment, the cyclic complex may be broken. Due to the hydrogen-bonding competition between two methanol molecules, re-forming of the cyclic structure within the **PQ-(MeOH)**$_2$ solvate becomes much slower than in the case of **PQ-(MeOH)$_1$**. When the cyclic structure becomes broken, various kinds of noncyclic separate hydrogen-bonded species may arise. After losing the cyclic structure in the case of **PQ-(MeOH)$_2$**, the hydrogen-bonding competition usually follows for 20−30 ps and, during that time, a new 1:1 cyclic hydrogen-bonded complex is re-formed. Also, during that period, the methanol molecule that had been originally included in the cyclic complex can be exchanged by the other methanol molecule. In other words, the "static" presence of the cyclic complex in the HBD distribution is the result of "dynamically" breaking and re-forming of the cyclic hydrogen-bonded complex due to a continuous exchange of one methanol molecule by the other.

Such analysis of the hydrogen-bonding dynamics within a solvate containing two molecules of methanol reveals one of the main differences between **PQ** and **7AI**. Most of the time, the **7AI-(MeOH)$_2$** solvate exists as an "eight-membered ring" complex. Such species possesses a rigid structure, retained by a network of strong hydrogen-bonds. In contrast to the **PQ-(MeOH)**$_2$ solvate, the hydrogen-bonding within the **7AI-(MeOH)**$_2$ does not undergo the exchange of methanol molecules between the solute "active sites". The hydrogen-bonding within the "eight-membered ring" structure is characterized by thermally activated continuous stretching and vibrations of the triply hydrogen-bonded ring, but full loss of such structure is extremely rare. The same structure of the complex could be detected without the exchange of methanol molecules for 100 ps. (It is instructive to remind in this context that the excited-state solvent rearrangement leading to ESDPT of **7AI** in methanol, has been found to occur in 140 ps.)[16] As a result, for the **7AI-(MeOH)**$_2$ solvate, the 1:1 cyclically hydrogen-bonded

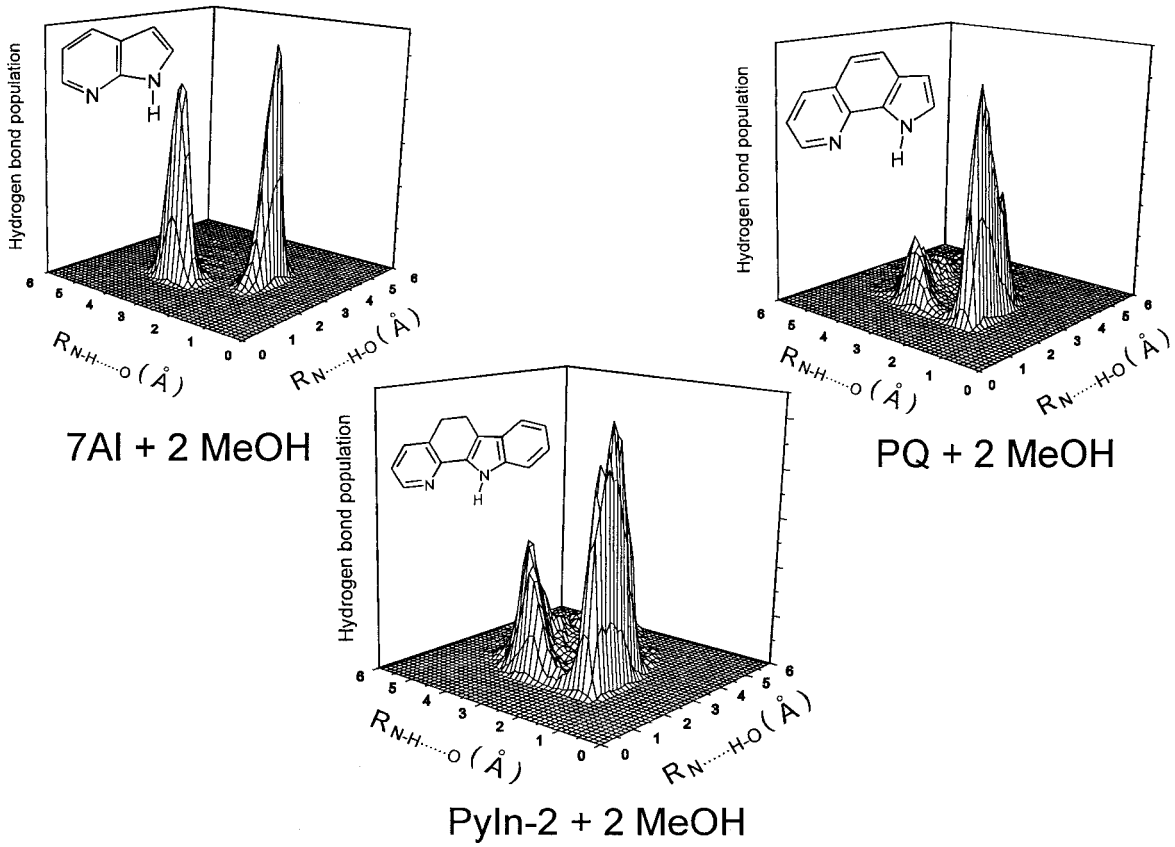

Figure 4. The results of MD simulations for **7AI**, **PQ**, and **PyIn-2** in *n*-hexane containing two molecules of methanol.

complex of **7AI** with one methanol is practically absent in the corresponding HBD distribution (Figure 4). The absence of a frequent exchange of two molecules of methanol within the **7AI**-(**MeOH**)$_2$ solvate can also be deduced from the presence of only two peaks in the HBD distribution. If the process of forming and breaking of various separately hydrogen-bonded species that differ from the "eight-membered ring" structure, had occurred during MD simulations, a nonzero hydrogen-bonding intensity could have been detected between the main peaks in the HBD distribution. In contrast to **7AI**, the effect is observed for **PQ**, where the occurrence of the broad intensity of hydrogen-bonding distribution around the main peaks reveals the presence of many intermediate hydrogen-bonded species.

The HBD distribution for **PyIn-2-(MeOH)$_2$** (Figure 4) reveals, in analogy with **PQ**, at least three different stable hydrogen-bonded solvates. Reconstruction of their structure results in the same kind of complexes as found for **PQ**: a cyclic doubly hydrogen-bonded species, found, on the average, for 15−26% of the time, and two noncyclic, separately hydrogen-bonded complexes. The predominant hydrogen-bonding occurs between the hydrogen atom of the solute pyrrole moiety and the methanol oxygen. The population of this complex corresponds to the main peak of the distribution. This result nicely agrees with our previous experimental observation that the ground-state hydrogen-bonding occurs preferentially to the NH group.[54] The second noncyclic complex is due mainly to hydrogen-bonding to the **PyIn-2** pyridine-type nitrogen atom. The fraction of this complex is about twice smaller than that of the former. The hydrogen-bonding dynamic behavior within the **PyIn-2-(MeOH)$_2$** solvate shows that neither a 1:1 cyclically bonded species nor a 1:2 "nine-membered ring" structure, the analogue of the "eight-membered ring" of **7AI** solvate, is found as a long-lived stable hydrogen-bonded complex. The hydrogen-bonding can be described in this case by, continuous and frequent, breaking and re-forming of separate hydrogen-bonds between the **PyIn-2** "active sites" and one of the two methanol molecules. Methanol−methanol hydrogen-bonding also occurs, but the main tendency is to form two independent strong hydrogen-bonds with the **PyIn-2** solute. What is interesting, a frequent exchange between two molecules of methanol in the **PyIn-2-(MeOH)$_2$** solvate occurs, and, as a result, many nonstable intermediate hydrogen-bonded species could be detected. This explains a high level of broad hydrogen-bonding intensity distribution in the middle region between the main peaks (Figure 4). Thus, **PyIn-2** can be treated as a structure intermediate between **7AI** and **PQ** with regard to the dynamic manner of hydrogen-bonding solvation, when two molecules of methanol are available. At 1:2 stoichiometry, the 1:1 cyclic, doubly hydrogen-bonded complexes become already less favorable, but stabilization due to the solvation via a network of hydrogen-bonds, which would result in a "nine-membered ring" structure, is not reached.

Figure 5 presents the HBD distributions for **7AI**, **PQ,** and **PyIn-2** solutes in bulk methanol. Upon passing from a dilute solution to a bulk solvent, growing of the intensity of solute−solvent hydrogen-bonding at a long-distance region in an HBD distribution has been observed, due to methanol molecules beyond the first solvation shell. Since we are not interested in analyzing this region, the corresponding intensity was cut off in order to improve the visibility of the most important parts of the distribution. In the solute−solvent hydrogen-bonding distribution for **7AI** in bulk methanol, two peaks can be observed. Their fwhm values increase, in comparison to the case of **7AI-(MeOH)$_2$**. Moreover, the maxima of both peaks are shifted toward a long-range distance region by comparison with the same peaks in dilute solution. Such kind of an HBD distribution cannot correspond to a complex with the "eight-membered ring" structure. By tracing the hydrogen-bonding dynamics of the **7AI**

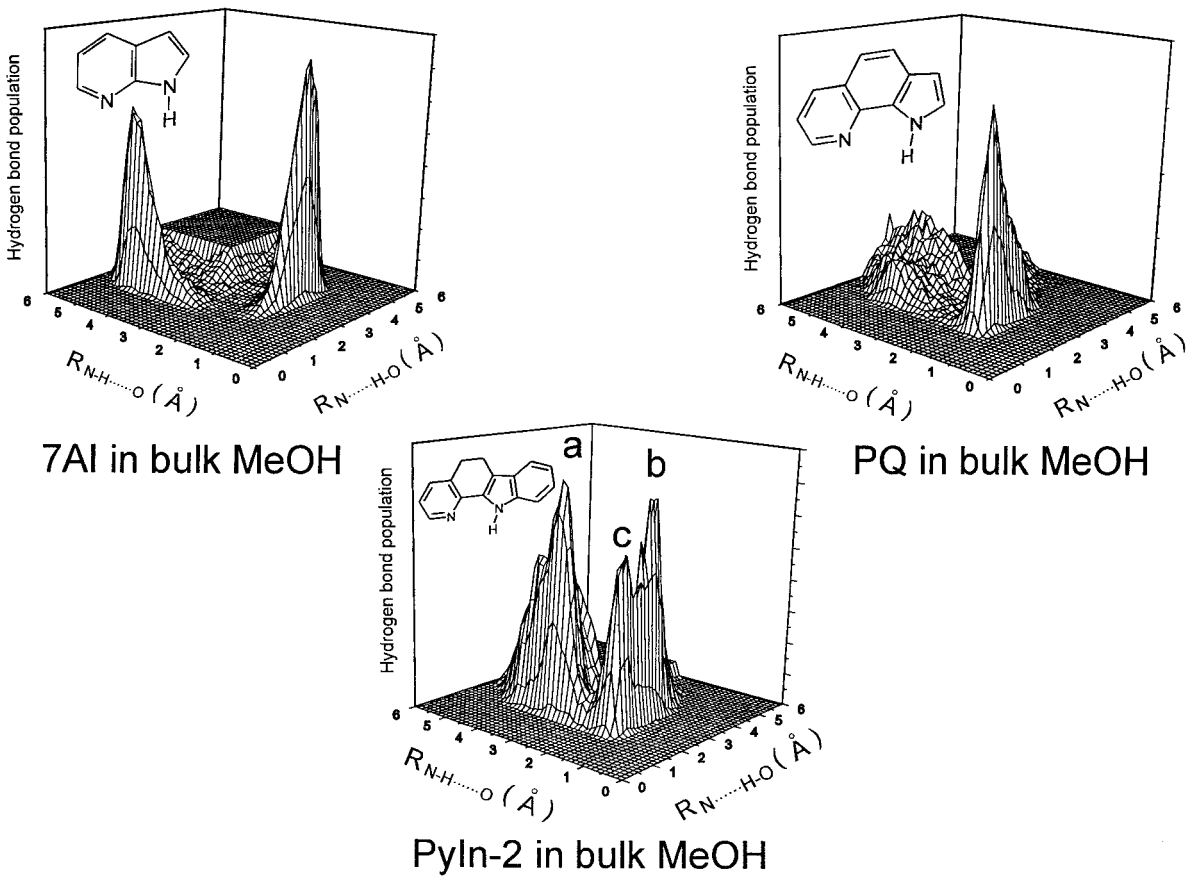

Figure 5. The results of MD simulations for **7AI**, **PQ**, and **PyIn-2** in bulk methanol.

solute in bulk methanol, this conclusion was confirmed. Both broad peaks correspond rather to a complex in which the solute is simultaneously hydrogen-bonded via its both "active sites" to two molecules of methanol, independently interacting with bulk methanol environment rather than with each other. These molecules are being periodically exchanged by methanol molecules from the bulk solvent. Thus, the **7AI** "eight-membered ring" complex has practically disappeared in bulk methanol. What is most important, for the case of the **7AI** solute in bulk methanol the equilibrium population of the 1:1 cyclic, doubly hydrogen-bonded complex was found to be smaller than 1%.

The HBD distribution for **PQ** in bulk methanol (Figure 5) is very similar to that obtained for **PQ-(MeOH)$_2$**. The maximum and the fwhm of the main peak remain unchanged in comparison to the 1:2 complex. Upon passing from a dilute solution to bulk methanol, the equilibrium between the 1:1 cyclic and various noncyclic hydrogen-bonded species is not significantly shifted toward the latter: The equilibrium population of the 1:1 cyclic complex was found to be equal to 24% and 35% for the two cutoff values, respectively. These values are only slightly smaller than those corresponding to the fraction of cyclic complexes in the case of dilute solution when only two molecules of methanol are available. Much more significant changes can be seen in the HBD distribution for the **PyIn-2** solute in bulk methanol. Again, as in the case of **PyIn-2-(MeOH)$_2$**, three peaks (labeled a, b, and c in Figure 5) are observed in the distribution. Reconstruction of the structure of the complexes, results in the same type of hydrogen-bonded species as in **PyIn-2-(MeOH)$_2$**. Peaks a and b correspond to noncyclic separate solute−solvent hydrogen-bonding, while peak c reflects the presence of 1:1 cyclic, doubly hydrogen-bonded species. Upon passing to bulk solvent, it is usually found that the peaks corresponding to separate solute−solvent hydrogen-bonding become shifted toward the long-distance region. This may be rationalized as due mainly to the hydrogen-bonding of the methanol molecule involved in the interaction with bulk environment. In the case of **PyIn-2** distribution in bulk methanol, such a long-distance shifting of the b peak results in the separation between the former and the c peak (cf., Figures 4 and 5). In a fashion much more spectacular than in **PQ**, upon passing from a dilute mixture solution to bulk solvent, the equilibrium population of the 1:1 cyclically doubly hydrogen-bonded complexes of the **PyIn-2** solute becomes reduced to 9−15%.

In ref 41, analogous HBD distribution, obtained by Monte Carlo simulations in bulk methanol, was presented for another of our molecules—**DPC**, a compound possessing the same topology of the "active hydrogen-bonding sites" as **PQ**. The fraction of the 1:1 cyclic species was not estimated, but, from the corresponding HBD distribution, three peaks, similar to those presented in Figure 5 for **PyIn-2**, can be clearly seen. For **DPC**, the hydrogen-bonding intensity under the peak corresponding to the cyclic complex dominates over the intensity of two other peaks. Thus, in bulk methanol, the **DPC** solute behaves similarly to **PQ**, which is in perfect agreement with experimental observations.[48,53]

We have also examined 1:*n* solute−solvent hydrogen-bonded solvates with *n* up to 5. When more hydrogen-bonding partners are available, a bifunctional solute molecule in dilute solution can exist in a wide range of hydrogen-bonded configurations. As a result, diffusive redistribution among different 1:*n* solute−solvent hydrogen-bonded species is possible. What is most interesting, the addition of subsequent molecules of methanol to a 1:2 solvate does not cause considerable changes in the hydrogen-bonding pattern in larger 1:*n* solvates. The most

dramatic changes in the HBD distribution are observed when the first two solvent molecules are added. Stepwise addition of the third, fourth, and fifth molecule of methanol produces no significant changes in the corresponding HBD distribution. Thus, if the breaking of the cyclic hydrogen-bonded structure in favor of other noncyclic species with a strong preference for two separate hydrogen-bonds is profitable, such tendency for the hydrogen-bonding rearrangement can be noticed already in dilute solution for a 1:2 solute−solvent stoichiometry.

The main conclusion which can be drawn from dilute solution simulations corroborates what has been usually postulated on the basis of experimental results obtained while adding small amounts of alcohol to a hydrocarbon solution:[46,48,53] When a bifunctional heteroazaaromatic molecule interacts with an hydrogen-bonding partner at 1:1 stoichiometry, the solute usually prefers forming a cyclic double hydrogen-bonded complex. This is the case for all the molecules under the present study.

Large differences between the three molecules start appearing already at 1:2 stoichiometry. One of the possible explanations for the observed differences between **7AI** and **PQ** may involve different topology of the solute "active sites". This different topology can lead to different geometrical arrangements of the hydrogen bonds between the solute and solvent molecules. The binding energy associated with the formation of the hydrogen-bonding was suggested as the key factor explaining the predominance of one species, cyclic or noncyclic, over the other one.[41] We calculated the energy of interaction between the solute and methanol in *n*-hexane as a sum of Coulomb and van der Waals contributions, averaged during a 500 ps MD simulation. The average pair-binding energy was found to be equal to 8.0 ± 1.0, 8.3 ± 0.5, and 8.7 ± 0.4 kcal/mol for **7AI**, **PyIn-2,** and **PQ**, respectively.

In the next step, we compared the MD results with those obtained by structure calculations. The ground-state optimized geometries and binding energies for 1:1 and 1:2 solute−methanol complexes were analyzed using DFT, an approach previously recommended for the analysis of hydrogen-bonding.[66−70] In all cases studied, two main kinds of solute−solvent complexes were usually observed: a π-complex and an hydrogen-bonded complex. Here, we focus our attention on the most stable hydrogen-bonded structure only. It has to be pointed out first that a solute−solvent interaction occurring upon complexation does not lead to significant geometry changes in the geometry of the solute, included in the complex, with respect to the geometry of the bare solute molecule. This result is important because a DFT-optimized geometry of a bare molecule was used for an MD representation of a solute in all our simulations (dilute mixture solution, bulk methanol, and water). The largest changes for the C−C and C−N bond lengths were found to be equal to 0.005...0.010 Å. The pyrrolic N−H bond length was found to be elongated by 0.019 Å for **PQ** and **PyIn-2** hydrogen-bonded solutes in both 1:1 and 1:2 complexes, and by 0.012 and 0.026 Å in **7AI-(MeOH)$_1$** and **7AI-(MeOH)$_2$** complexes, respectively. Figures 6 and 7 present the B3LYP/6-31G(d,p) energy-minimized geometries of the ground state of various types of **7AI, PQ,** and **PyIn-2** methanol complexes. The geometry optimization of a hydrogen-bonded complex for a 1:1 stoichiometry was always converging to a cyclic, double hydrogen-bonded structure. The two shortest hydrogen-bonds, practically equal to each other, were found in **PQ-(MeOH)$_1$**. On the contrary, the longest hydrogen-bonds were observed for the **7AI-(MeOH)$_1$** structure. In the case of **PyIn-2-(MeOH)$_1$** complex, the two hydrogen-bonds were found to be only slightly elongated in comparison with the **PQ** case: the N−H···O bond

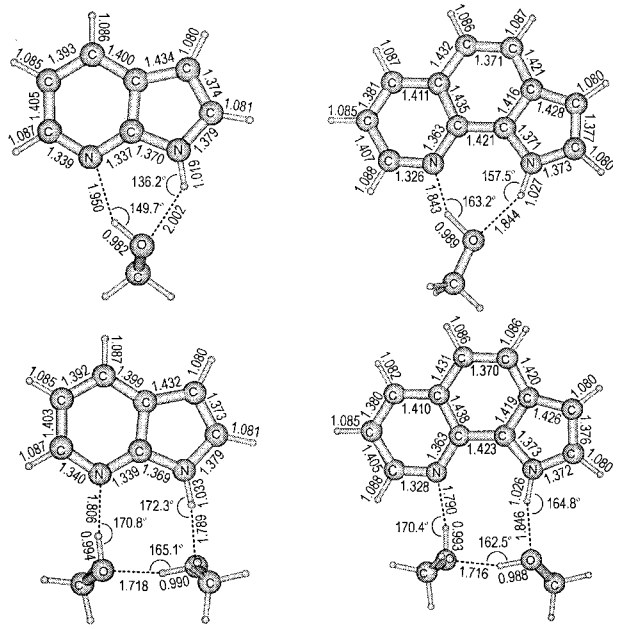

Figure 6. B3LYP/6-31G(d,p) geometries of 1:1 and 1:2 cyclic complexes of **7AI** and **PQ** with methanol.

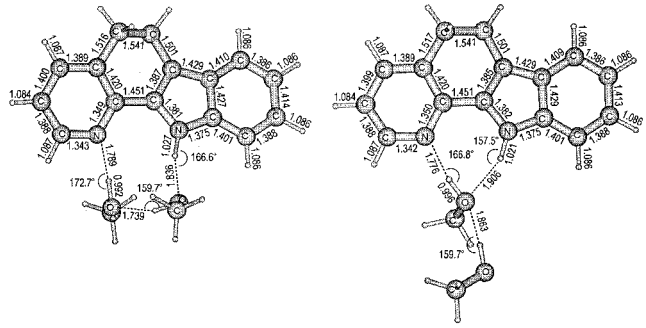

Figure 7. B3LYP/6-31G(d,p) geometries of two types of 1:2 complexes of **PyIn-2** with methanol.

is 1.867 Å and the N···H−O bond is 1.851 Å, to be compared with the values of 1.844 and 1.843 Å in **PQ**. Bare **PyIn-2** solute, as well as the same solute included in the hydrogen-bonded complex, was found to be slightly nonplanar. The angle between the pyridine and indole moieties is about 12°. Other relevant data are given in Table 2. An important finding is that in **PQ** and **PyIn-2** complexes, which both possess a similar topology of "active hydrogen-bonding sites", the two hydrogen-bonds were found to be more linear than in the **7AI-(MeOH)$_1$** complex. A linear hydrogen-bond is energetically preferred on the basis of simple electrostatic and hybridized valence bond considerations. Furthermore, the strength of a hydrogen-bonding association is usually correlated with simple hydrogen-bonding geometrical parameters such as X−H···Y bond length and angle. Thus, the largest deviations from the idealized hydrogen-bonded geometry within the series of three complexes occur for **7AI**.

The B3LYP/6-31G(d,p) binding energies, including the ZPE and BSSE corrections to ΔE, were found to be equal to 7.8, 8.1, and 9.9 kcal/mol for the 1:1 solute:methanol complexes with **7AI**, **PyIn-2,** and **PQ**, respectively. Both absolute and relative binding energies obtained by MD and DFT calculations agree very well. Thus, **PQ** is predicted to give the strongest complex with **MeOH** by both methods. On the other hand, the hydrogen-bonding in the **7AI-(MeOH)$_1$** complex is found to be the weakest. Moreover, the computed binding energies and the values of ΔH, experimentally determined enthalpies of the

TABLE 2: Hydrogen-Bonding Parameters Computed Using B3LYP/6-31G(d,p) for Three Types of Complexes with Methanol (ΔH, experimental values for 1:1 complex formation; see Figures 6 and 7 for details)

	$R_{N\cdots H-O}$ (Å)	$\angle_{N\cdots H-O}$ (deg)	$R_{N-H\cdots O}$ (Å)	$\angle_{N-H\cdots O}$ (deg)	ΔE (kcal/mol)	ΔH (kcal/mol)
			A: Cyclic 1:1 Species			
PQ + 1 MeOH	1.843	163.2	1.844	157.5	−9.9	-9.2 ± 0.7^a
PyIn2 + 1 MeOH	1.851	164.1	1.867	158.6	−8.1	-8.7 ± 0.2^b
7AI + 1 MeOH	1.950	149.7	2.002	136.2	−7.8	-6.3 ± 1.5^c
			B: Cyclic 1:1 Species Solvated by a Second Methanol Molecule			
PQ + 2 MeOH	1.754	166.8	1.898	154.7	−13.3	
PyIn2 + 2 MeOH	1.776	168.8	1.906	157.5	−11.4	

	$R_{N\cdots H-O}$ (Å)	$\angle_{N\cdots H-O}$ (deg)	$R_{O\cdots H-O}$ (Å)	$\angle_{O\cdots H-O}$ (deg)	$R_{N-H\cdots O}$ (Å)	$\angle_{N-H\cdots O}$ (deg)	ΔE (kcal/mol)
			C: Cyclic, Triply Hydrogen-Bonded Structures				
PQ + 2 MeOH	1.790	170.4	1.716	162.5	1.846	164.8	−15.1
PyIn2 + 2 MeOH	1.789	172.7	1.739	159.7	1.836	166.6	−14.8
7AI + 2 MeOH	1.806	170.8	1.718	165.1	1.789	172.3	−18.4

[a] Complex with *n*-butanol in *n*-hexane. [b] Methanol complex in *n*-hexane.[54] [c] Methanol complex in cyclohexane.[26]

hydrogen-bonding association, are in excellent agreement. The enthalpy for the complex formation between **7AI** and **MeOH** in a cyclohexane solution, was reported by Chou and co-workers as -6.3 ± 1.5 kcal/mol.[26] The ΔH value for **PyIn-2-(MeOH)$_1$** complex in *n*-hexane was estimated to be -8.7 ± 0.2 kcal/mol.[54] We also determined, using previously reported[48] spectroscopic titration results, the enthalpy of the hydrogen-bonding association between **PQ** and *n*-butanol in *n*-hexane solution, which was found to be -9.2 ± 0.7 kcal/mol. The stoichiometry is 1:1 and it is expected that the hydrogen-bonded complex corresponds to a cyclic structure. Thus, both experimental and theoretical findings provide substantial evidence that the strength of hydrogen-bonding decreases in the order **PQ-(MeOH)$_1$** > **PyIn-2-(MeOH)$_1$** > **7AI-(MeOH)$_1$**.

Chou and co-workers reported a significant increase in the experimental and calculated absolute ΔH values for a 1:1 **7AI**-(acetic acid or lactam) complex with respect to the **7AI-(MeOH)$_1$** structure.[25−27] A natural explanation was that the large ΔH for the **7AI-(CH$_3$COOH)$_1$** complex is due to the possibility of the adjustment of both distances and both angles within the doubly hydrogen-bonded configuration toward an idealized structure, in which the N−H···O and N···H−O bonds would be linear. This becomes possible due to the change of the topology of the "solvent hydrogen-bonding sites". In line with the above discussion, the additional exothermicity for **PQ-(MeOH)$_1$** complex formation by comparison with **7AI-(MeOH)$_1$** can be regarded as a result of an "adjustment" of the topology of the "solute hydrogen-bonding sites" in order to approach the optimal doubly hydrogen-bonded structure.

Thus, the results of our DFT study answer the questions about different stabilities of the hydrogen-bonded complexes with solutes possessing different topology of the "hydrogen-bonding sites", i.e., **PQ** with respect to **7AI**. However, such an analysis cannot clearly explain the different stabilities of the same type of complexes within a series of similar compounds with an identical mutual configuration of both hydrogen-bonding centers. For three of our compounds—**PQ**, **TPC,** and **PC**—the HF/6-311G(d,p) binding energies for a 1:1 cyclic doubly hydrogen-bonded complex with methanol were found to be equal to 6.6, 6.5, and 6.2 kcal/mol, respectively. It was not surprising to find differences in absolute binding energies computed by the DFT and HF approaches, i.e., with and without taking into account the electron correlation effects. Analogous results have been reported previously.[36] A more important finding was that the binding energies in **PQ**, **TPC,** and **PC** complexes were found to be very similar. On the other hand, we have experimentally shown that in bulk alcohol the equilibrium population of the cyclic versus noncyclic hydrogen-bonded solute−solvent species varies strongly across the series.[48] The difference between the energies of formation of **PQ-(MeOH)$_1$** and **PyIn-2-(MeOH)$_1$** complexes, obtained using B3LYP/6-31G(d,p), is also of little value when it comes to predicting the ratio of the cyclic/noncyclic complexes in a bulk alcohol.

As mentioned previously, an intriguing result of the MD analysis was the finding that, among 1:2 solute−solvent complexes with methanol in *n*-hexane, **7AI**, **PyIn-2,** and **PQ** show completely different structure and hydrogen-bonding dynamics. Moreover, such a surprising behavior may be regarded as a key feature enabling better insight into the solvation of DNA base pair-like compounds in bulk environment. The structure of the 1:2 solute−methanol hydrogen-bonded species can usually be reconstructed from the corresponding HBD distribution. Unfortunately, in some cases a direct determination of the geometry of the 1:2 complex is not possible because of difficulties in extracting the exact values for the peaks corresponding to such a complex from an HBD distribution. Moreover, the energy difference between the "eight-membered ring"-like structure, as in the **7AI** case, and the other possible 1:2 cyclic/or noncyclic hydrogen-bonded species could not be clearly obtained by our MD analysis.

We have therefore explored various 1:2 solute−methanol complexes on the DFT level. Two kinds of hydrogen-bonded species were examined. The first was a cyclic, triply hydrogen-bonded complex containing two methanol molecules arranged in a closed ring structure (Figures 6 and 7). The second was a complex also containing two methanol molecules, but in which one methanol is doubly hydrogen-bonded to a solute in a cyclic fashion, with another methanol hydrogen-bonded to the first methanol molecule (Figure 7, right). Other possible hydrogen-bonded species as well as the π-complexes were not considered in the present work.

B3LYP/6-31G(d,p) optimized geometries of cyclic, triply hydrogen-bonded **7AI-(MeOH)$_2$** and **PQ-(MeOH)$_2$** complexes are presented in Figures 6−7 and Table 2. In the **7AI** case two solute−solvent hydrogen-bonds within the "eight-membered ring" structure become shorter than those in the **7AI-(MeOH)$_1$** complex. The values of both hydrogen-bond angles approach the ideal value of 180°. It is instructive to analyze the N−H···O and N···H−O distances between the solute and solvent "active hydrogen-bonding sites" for each solvent molecule in the optimized "eight-membered ring" structure. In the case of **7AI-(MeOH)$_2$** complex, for the first methanol molecule, presented in Figure 6 on the left, the N···H−O hydrogen-bond is 1.81 Å while the N−H···O distance between the oxygen atom of the

same methanol molecule and the pyrrolic hydrogen atom is 3.16 Å. For the second methanol molecule, the corresponding N−H···O bond and the N···H−O distance are found to be 1.79 and 3.38 Å, respectively. Thus, the optimal B3LYP/6-31G(d,p) "eight-membered ring" structure corresponds to two points on the HBD distribution. We may now compare the hydrogen-bond distances with those obtained by MD simulations. Figure 4 and Table 1 show that the most probable structure for the **7AI-(MeOH)$_2$** complex, according to the MD simulation results, has the HBD coordinates equal to 1.89 and 3.45 Å, and 3.19 and 1.89 Å, respectively. Thus, the HBD distribution for the **7AI-(MeOH)$_2$** complex really corresponds to an "eight-membered ring" structure.

In the **PQ-(MeOH)$_2$** and **PyIn-2-(MeOH)$_2$** cyclic "nine-membered ring" structure, the rearrangement of the closed network of three hydrogen-bonds takes place also toward the idealized hydrogen-bond parameters (Figures 6 and 7). The B3LYP/6-31G(d,p) binding energies of the cyclic, triply hydrogen-bonded complexes of **7AI**, **PyIn-2** and **PQ** with two methanol molecules were found to be equal to 18.4, 14.8 and 15.1 kcal/mol, respectively. Thus, for 1:2 cyclic, triply hydrogen-bonded complexes, the opposite tendency than that obtained for a 1:1 complex could be observed across the series. The "eight-membered ring" structure, present in **7AI** complex, is found to be the most stable one. The B3LYP/6-31G(d,p) binding energies for the second kind of 1:2 hydrogen-bonded species, similar to the **PyIn-2-(MeOH)$_2$** complex presented in Figure 7, were calculated by using an analogous procedure. The binding energies for this type of complexes of **PyIn-2** and **PQ** with two methanol molecules were found to be 11.4 and 13.3 kcal/mol, respectively. In the case of **7AI-(MeOH)$_2$**, such noncyclic structure has not been found. Geometry optimizations for **7AI-(MeOH)$_2$** starting with various initial configurations were attempted, including the configuration composed of the optimized 1:1 **7AI-MeOH** cyclic, double hydrogen-bonded structure with the second methanol molecule near the optimized complex. Independent from the starting point, the geometry optimization of **7AI-(MeOH)$_2$** was always converging to the same configuration—the "eight-membered ring" structure (Figure 6). Thus, in the case of **7AI-(MeOH)$_2$** it appears that only one energy minimum exists on a global potential energy surface, corresponding to the most stable structure.

For the three bifunctional solute molecules under study, the triple hydrogen-bonded structure, arranged in the closed hydrogen-bond network ring, was found to be more stable than the other possible hydrogen-bonded configuration (Figure 7). It is known[32,71−72] that a multiple, cyclic hydrogen-bonding, even including a pseudo hydrogen-bonding with a hydrogen atom attached to an aromatic carbon, is in many cases found energetically more preferable than a separate hydrogen-bonding at the same stoichiometry. Thus, to some extent, such results could have been expected. On the other hand, according to our MD simulations for the dilute solution at 1:2 stoichiometry, the cyclic, closed triply hydrogen-bonded structure was found to be most stable only for **7AI** solute. In cases of **PQ** and **PyIn-2**, the 1:1 cyclic, double hydrogen-bonded complex was found most of the time even at the 1:2 solute−solvent stoichiometry. Thus, the DFT results for the association reaction within the series reveal the tendencies for the structure and hydrogen-bonding stability of the complex. However, due to the neglect of bulk solvent effects, these tendencies cannot be extrapolated to the bulk environment. In other words, these findings reflect a situation when our treatment of all observed differences is due to only the total energy cost of the formation of an isolated complex, either in a vacuum or in a hydrocarbon solvent. Such approach seems to be too simple and a separate examination of the enthalpy and the entropy contributions is necessary.

Finally, we tried to examine the predictive power of our MD approach using water as another hydrogen-bonding solvent containing multiple hydrogen-bonding centers. The MD simulations were performed for dilute mixture solutions in *n*-hexane as well as for the bulk solvent. Figure 8 presents the HBD distribution for complexes of **7AI**, **PQ,** and **PyIn-2** with one water molecule. In the cases of **PQ-(H$_2$O)$_1$** and **PyIn-2-(H$_2$O)$_1$**, the corresponding HBD distribution is in many aspects very similar to that obtained for methanol. The cyclic, doubly hydrogen-bonded complex is found most of the time for both solutes. The structure of the complex, containing one water molecule, is also similar, in terms of the average hydrogen-bond distances and the corresponding fwhm values, to the 1:1 complex with methanol (Table 1). There is a small tendency of shortening of the N···H−O bond length by comparison with the same hydrogen-bond length in the case of methanol. The relative fraction of the cyclic, doubly hydrogen-bonded **PQ-(H$_2$O)$_1$** and **PyIn-2-(H$_2$O)$_1$** complexes is found to be the same as that of the cyclic complex with methanol within the error inherent in such an analysis. The most significant changes were observed for the **7AI-(H$_2$O)$_1$** HBD distribution, which was found to exhibit a considerable broadening for the hydrogen-bonding intensity along the N−H···O coordinate and a simultaneous shortening of the distance along the N···H−O direction. Although the relative fraction for the cyclic **7AI-(H$_2$O)$_1$** complex is found practically the same as that of the cyclic complex with one methanol molecule, the double hydrogen-bonded structure with one water molecule is somewhat less rigid than the **7AI-(MeOH)$_1$** complex. The HBD distribution in Figure 8 reveals another broad peak due to a separate hydrogen-bonding between the pyridine-type nitrogen atom of **7AI** and one of the two hydrogen atoms of the water molecule.

Figure 9 presents the HBD distribution for complexes of **7AI**, **PQ,** and **PyIn-2** with water at 1:2 stoichiometry. The corresponding distributions are very similar to the case of methanol presented in Figure 4. For **7AI-(H$_2$O)$_2$**, most of the time the "eight-membered ring" structure is found, in analogy with **7AI-(MeOH)$_2$** solvate. In the former case, the fwhm values for both peaks decrease by comparison with the HBD distribution of Figure 4. Thus, the "eight-membered ring" structure for the **7AI-(H$_2$O)$_2$** solvate should be more rigid than **7AI-(MeOH)$_2$**. Upon passing from methanol to water as solvent the relative population for the 1:1 cyclic double hydrogen-bonded complexes significantly decreases (Table 1).

The hydrogen-bonding dynamics within the **PQ-(H$_2$O)$_2$** and **PyIn-2-(H$_2$O)$_2$** solvates becomes complicated due to the hydrogen-bonding nature of water. As a result, a high level of the hydrogen-bonding intensity between the main peaks in the HBD distribution is observed, due to various intermediate intermolecularly hydrogen-bonded species. Nevertheless, the relative population of the 1:1 cyclic, double hydrogen-bonded complex remains approximately the same as in the case of methanol (Table 1). The analysis of the 1:2 solute−water solvate reveals a different response of each chromophore to adding the second solvent molecule to the system. However, in terms of structural rearrangement upon the addition of the second solvent molecule both methanol and water solvents exhibit a very similar behavior. Thus, this tendency is rather an intrinsic property of the particular bifunctional heteroazaaromatic solute molecule.

Figure 10 presents the HBD distributions for **7AI**, **PQ,** and **PyIn-2** in bulk water. Comparing both sets of the HBD

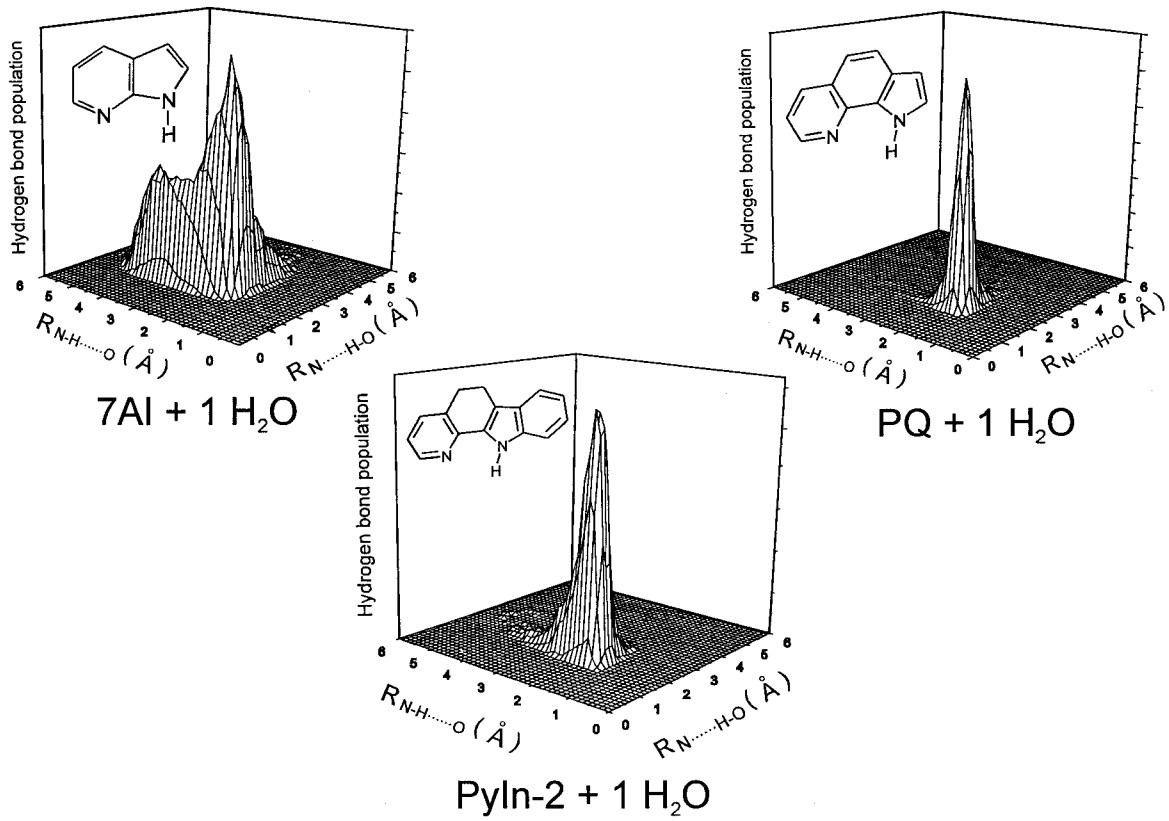

Figure 8. The results of MD simulations for **7AI**, **PQ**, and **PyIn-2** in *n*-hexane containing one molecule of water.

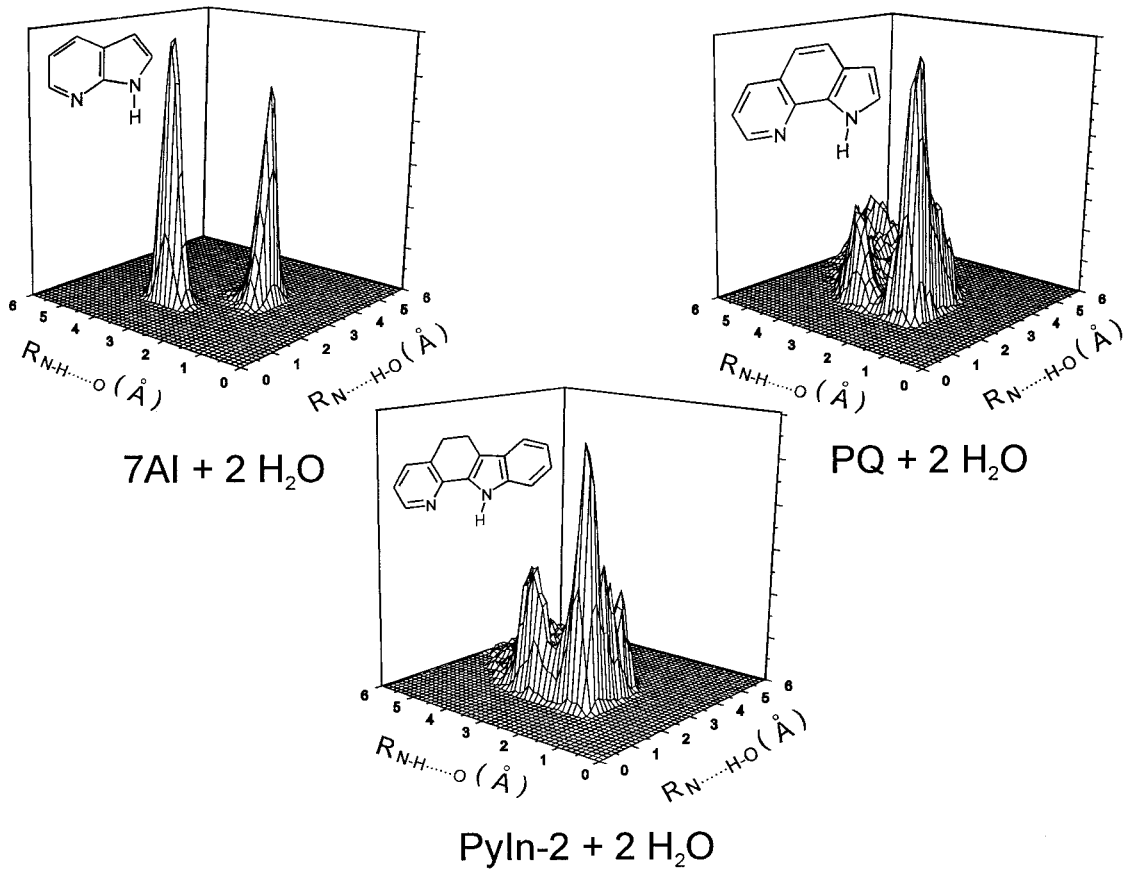

Figure 9. The results of MD simulations for **7AI**, **PQ**, and **PyIn-2** in *n*-hexane containing two molecules of water.

distributions for bulk methanol and water (Figures 5 and 10), one may see that both distributions for **7AI** are very similar. Thus, the structure of the **7AI** solvate in bulk water should be similar to the one in bulk methanol. In bulk water, the solvent molecules occupy the "active hydrogen-bonding sites" of **7AI** by means of independent separate hydrogen-bondings. Similar

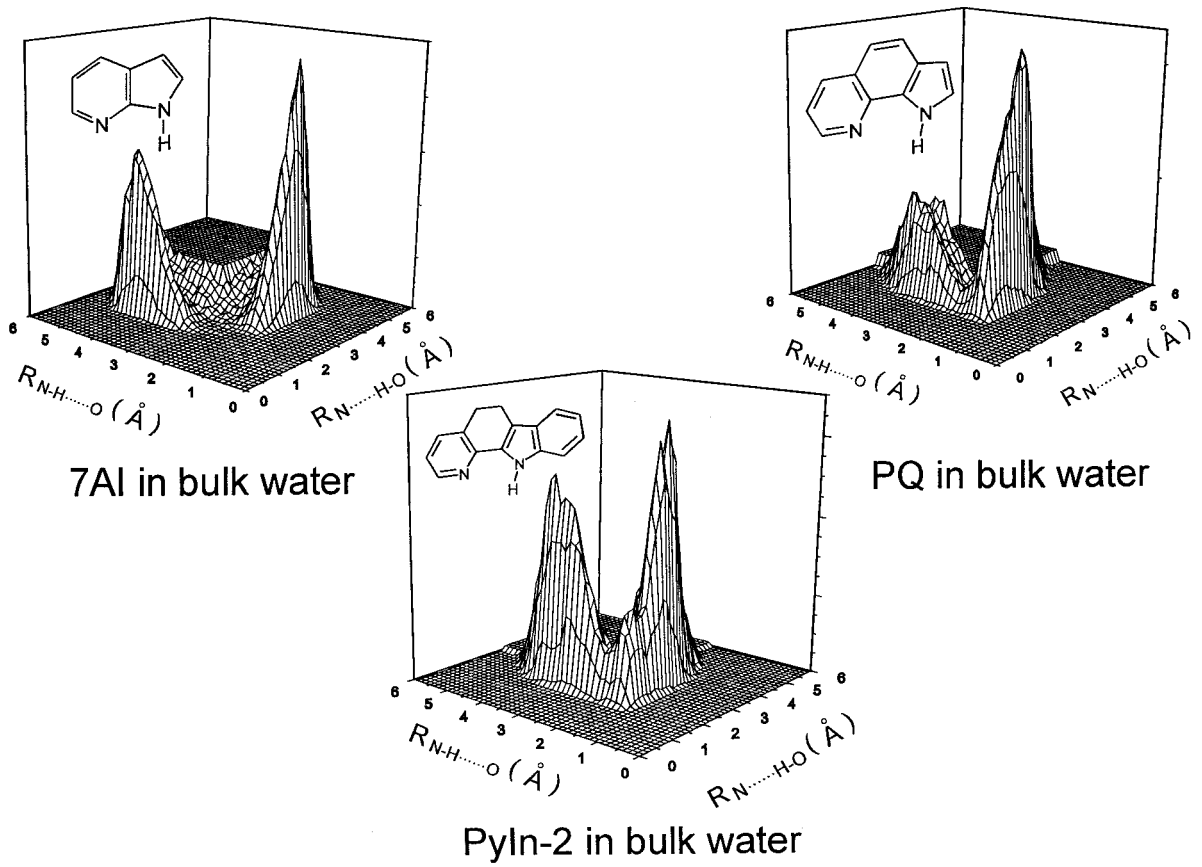

Figure 10. The results of MD simulations for **7AI**, **PQ**, and **PyIn-2** in bulk water.

changes are observed in the HBD distribution for **PQ** and **PyIn-2** in bulk water. The analysis of the redistribution of the hydrogen-bonding intensities for the three peaks (a, b, and c in Figure 5), corresponding to three differently hydrogen-bonded species, shows that the equilibrium between the 1:1 cyclic, doubly hydrogen-bonded complex and the two other separately hydrogen-bonded species (independent hydrogen-bondings via both solute "active sites" − N and N−H) is strongly shifted toward decrease in the relative fraction of the cyclic hydrogen-bonded structure. The equilibrium population of the 1:1 cyclic, doubly hydrogen-bonded species for **PQ** and **PyIn-2** in bulk water is found to be 3.5 and 3 times smaller than that of the cyclic complex in bulk methanol (Table 1). For **7AI** in bulk water this tendency is even stronger. Thus, an extensive hydrogen-bonding nature of water results in a large solvent self-aggregation and prevents the formation of the cyclic hydrogen-bonded structure.

4. Summary and Conclusions

The experimentally observed differences in the structure and relative populations of various type of intermolecular hydrogen-bonded complexes with three different azaaromatic molecules, **7AI**, **PyIn-2,** and **PQ** were nicely reproduced by DFT and molecular dynamics calculations. The DFT results correctly predict the trends along the series, but are of rather limited use for the estimation of relative populations of different solvates. On the contrary, MD results show that this approach is suitable for quantitative, or at least semiquantitative predictions. It would be particularly interesting to verify such predictions regarding the structure of water solvates, which have not been studied yet (**PyIn-2** and **PQ)**, or for which the interpretation remains controversial (**7AI**).

An intriguing difference was found between **PQ** and **PyIn-2**. The local topologies of the hydrogen-bonding sites of both molecules are similar; however, the population of the cyclic species in bulk alcohol for **PQ** is at least four times greater than the corresponding population for **PyIn-2**.[48] Naturally, "very similar topology" does not mean "completely identical": there are small differences in the structure of the double hydrogen-bonding. There are also small differences in the electronic density distribution and, as a result, the strength of hydrogen bonds may be different. **PyIn-2** is not flat. The calculated angle of twisting between the pyridine and the pyrrole moieties is about 12°. This twisting can facilitate formation of separate hydrogen bonds with the solvent. **PQ** and **PyIn-2** differ also with respect to one another in terms of rigidity. Thus, these small structural differences in the local topology can result in different hydrogen-bonding ability and cause large variations of the relative ground-state populations of the cyclic species in bulk solvent. Interestingly, MD simulations are able to reproduce these differences.

Our MD simulations confirm the experimental results and show that **PQ** and related compounds, possessing the same structural motif of the solute "active sites", are really a new class of heteroazaaromatic compounds in which the topology of the hydrogen-bonding centers is more favorable for the formation of the cyclic species in bulk alcohol and water than the corresponding topology of the **7AI** chromophore.

Acknowledgment. This work has been financed, in part, by the U.S.−Polish Maria Skłodowska-Curie Joint Fund II (Grant No. 97-305). We are grateful to Adam Fedorowicz for a helpful discussion concerning technical details of the GROMOS96 program package.

References and Notes

(1) (a) Miyasaka, H.; Tabata, A.; Kamada, K. N.; Mataga, N. *J. Am. Chem. Soc*. **1993**, *115*, 7335. (b) Martin, M. M.; Miyasaka, H.; Karen, A.; Mataga, N. *J. Phys. Chem.* **1985**, *89*, 182. (c) Ikeda, N.; Miyasaka, H.; Okada, T.; Mataga, N. *J. Am. Chem. Soc*. **1983**, *105*, 5206. (d) Martin, M. M.; Ikeda, N.; Okada, T.; Mataga, N. *J. Phys. Chem.* **1982**, *86*, 4148. (e) Martin, M. M.; Ware, W. R. *J. Phys. Chem*. **1978**, *82*, 2770. (f) Ikeda, N.; Okada, T.; Mataga, N. *Chem. Phys. Lett.* **1980**, *69*, 251. (g) Ikeda, N.; Okada, T.; Mataga, N. *Bull. Chem. Soc. Jpn.* **1981**, *54*, 4, 1025. (h) Mataga, N.; Torihashi, Y.; Kaifu, Y. Z. *Phys. Chem. (Frankfurt/Main)* **1962**, *34*, 379. (i) Mataga, N. *Bull. Chem. Soc. Jpn.* **1958**, *31*, 481. (i) Mataga, N.; Tsuno, S. *Bull. Chem. Soc. Jpn.* **1957**, *30*, 711. (j) Mataga, N.; Tsuno, S. *Naturwissenschaften* **1956**, *10*, 305.

(2) Rehm, D.; Weller, A. *Isr. J. Chem.* **1970**, *8*, 259.

(3) (a) Kikuchi, K.; Watarai, H.; Koizumi, M. *Bull. Chem. Soc. Jpn.* **1973**, *46*, 749. (b) Yamamoto, S.; Kikuchi, K.; Kokubun, H. *Ibid*. **1976**, *49*, 2950.

(4) (a) Waluk, J.; Komorowski, S. J.; Herbich, J. *J. Phys. Chem*. **1986**, *90*, 3868. (b) Waluk, J.; Komorowski, S. J. *Chem. Phys. Lett*. **1987**, *133*, 368. (c) Waluk, J.; Komorowski, S. J. *J. Mol. Struct*. **1986**, *142*, 159.

(5) Taylor, C. A.; El-Bayoumi, M. A.; Kasha, M. *Proc. Natl. Acad. Sci. U.S.A.* **1969**, *63*, 253.

(6) Douhal, A.; Kim, S. K.; Zewail, A. H. *Nature* **1995**, *378*, 260.

(7) Folmer, D. E.; Poth, L.; Wisniewski, E. S.; Castleman, A. W., Jr. *Chem. Phys. Lett.* **1998**, *287*, 1.

(8) Lopez-Martens, R.; Long, P.; Solgadi, D.; Soep, B.; Syage, J.; Millie, Ph. *Chem. Phys. Lett.* **1997**, *273*, 219.

(9) Fiebig, T.; Chachissvilis, M.; Manger, M.; Zewail, A. H.; Douhal, A.; Garcia-Ochoa, I.; de La Hoz Ayuso, A. *J. Phys. Chem. A* **1999**, *103*, 7419.

(10) Chachissvilis, M.; Fiebig, T.; Douhal, A.; Zewail, A. H. *J. Phys. Chem. A* **1998**, *102*, 669.

(11) (a) Takeuchi, S.; Tahara, T. *J. Phys. Chem. A* **1998**, *102*, 7740. (b) *Chem. Phys. Lett.* **1997**, *277*, 340.

(12) Smirnov, A. V.; English, D. S.; Rich, R. L.; Lane, J.; Teyton, L.; Schwabacher, A. W.; Luo, S.; Thornburg, R. W.; Petrich, J. W. *J. Phys. Chem. B* **1997**, *101*, 2758.

(13) Avouris, P.; Yang, L. L.; El-Bayoumi, M. A. *Photochem. Photobiol.* **1976**, *24*, 211.

(14) McMorrow, D.; Aartsma, T. J. *Chem. Phys. Lett.* **1986**, *125*, 581.

(15) Moog, R. S.; Bovino, S. C.; Simon, J. D. *J. Phys. Chem.* **1988**, *92*, 6545.

(16) Konijnenberg, J.; Huizer, A. H.; Varma, C. A. G. O. *J. Chem. Soc., Faraday Trans. 2* **1988**, *84*, 1163.

(17) Moog, R. S.; Maroncelli, M. *J. Phys. Chem.* **1991**, *95*, 10359.

(18) Herbich, J.; Sepioł, J.; Waluk, J. *J. Mol. Struct.* **1984**, *114*, 329.

(19) Chapman, C. F.; Maroncelli, M. *J. Phys. Chem*. **1992**, *96*, 8430.

(20) Chen, Y.; Gai, F.; Petrich, J. W. *J. Am. Chem. Soc.* **1993**, *115*, 10158.

(21) Chen, Y.; Gai, F.; Petrich, J. W. *Chem. Phys. Lett*. **1994**, *222*, 329.

(22) Chen, Y.; Rich, R. L.; Gai, F.; Petrich, J. W. *J. Phys. Chem.* **1993**, *97*, 1770.

(23) Chou, P.-T.; Martinez, M. L.; Cooper, W. C.; Collins, S. T.; McMorrow, D. P.; Kasha, M. *J. Phys. Chem.* **1992**, *96*, 5203.

(24) Bulska, H.; Grabowska, A.; Pakuła, B.; Sepioł, J.; Waluk, J.; Wild, U. P. *J. Lumin.* **1984**, *29*, 65.

(25) Chang, C.-P.; Wen-Chi, H.; Meng-Shin, K.; Chou, P.-T.; Clements, J. H. *J. Phys. Chem.* **1994**, *98*, 8801.

(26) Chou, P.-T.; Wei, C.-Y.; Chang, C.-P.; Meng-Shin, K. *J. Phys. Chem.* **1995**, *99*, 11994.

(27) Chou, P. T.; Wei, C. Y.; Chang, C. P.; Chiu, C. H. *J. Am. Chem. Soc.* **1995**, *117*, 7259.

(28) Chou, P. T.; Liao, J.-H.; Wei, C. Y.; Yang, C.-Y.; Yu, W.-S.; Chou, Y.-H. *J. Am. Chem. Soc.* **2000**, *122*, 986.

(29) Hetherington, W. M., III.; Micheels, R. M.; Eisenthal, K. B. *Chem. Phys. Lett.* **1979**, *66*, 230.

(30) Share, P. E.; Sarisky, M. J.; Pereira, M. A.; Repinec, S. T.; Hochstrasser, R. M. *J. Lumin.* **1991**, *48/49*, 204.

(31) Bulska, H.; Chodkowska, A. *J. Am. Chem. Soc*. **1980**, *102*, 3259.

(32) Nakajima, A.; Hirano, M.; Hasumi, R.; Kaya, K.; Watanabe, H.; Carter, C. C.; Williamson, J. M.; Miller, T. A. *J. Phys. Chem. A* **1997**, *101*, 392.

(33) Huang, Y.; Sulkes, M. *J. Phys. Chem.* **1996**, *100*, 4734.

(34) Kim, S. K.; Bernstein, E. R. *J. Phys. Chem.* **1990**, *94*, 3531.

(35) Fuke, K.; Yoshiuchi, H.; Kaya, K. *J. Phys. Chem.* **1984**, *88*, 5840.

(36) Gordon, M. *J. Phys. Chem.* **1996**, *100*, 3974.

(37) Chaban, G. M.; Gordon, M. S. *J. Phys. Chem. A* **1999**, *103*, 185.

(38) Shukla, M. K.; Mishra, P. C. *Chem. Phys.* **1998**, *230*, 187.

(39) Graña, A. M. *J. Mol. Structure (THEOCHEM)* **1999**, *466*, 145.

(40) Douhal, A.; Guallar, V.; Moreno, M.; Lluch, J. M. *Chem. Phys. Lett.* **1996**, *256*, 370.

(41) Mente, S.; Maroncelli, M. *J. Phys. Chem. A* **1998**, *102*, 3860.

(42) Mente, S.; Frankland, S. J. V.; Reynolds, L.; Maroncelli, M. *Chem. Phys. Lett.* **1998**, *293*, 515.

(43) Guallar, V.; Batista, V. S.; Miller, W. H. *J. Chem. Phys.* **1999**, *110*, 9922.

(44) Chang, C.; Shabestary, N.; El-Bayoumi, M. A. *Chem. Phys. Lett.* **1980**, *75*, 107.

(45) Waluk, J.; Grabowska, A.; Pakuła, B.; Sepioł, J. *J. Phys. Chem.* **1984**, *88*, 1160.

(46) Waluk, J.; Komorowski, S. J.; Herbich, J. *J. Phys. Chem.* **1986**, *90*, 3868.

(47) Fuke, K.; Kaya, K. *J. Phys. Chem.* **1989**, *93*, 614.

(48) Kyrychenko, A.; Herbich, J.; Izydorzak, M.; Wu, F.; Thummel, R. P.; Waluk, J. *J. Am. Chem. Soc.* **1999**, *121*, 11179.

(49) Kyrychenko, A.; Herbich, J.; Wu, F.; Thummel, R. P.; Waluk, J. *J. Am. Chem. Soc.* **2000**, *122*, 2818.

(50) Marks, D.; Zhang, H.; Borowicz, P.; Waluk, J.; Glasbeek, M. *J. Phys. Chem. A* **2000**, *104*, 7167.

(51) Kyrychenko, A.; Herbich, J.; Izydorzak, M.; Gil, M.; Dobkowski, J.; Wu, F.; Thummel, R. P.; Waluk, J. *Isr. J. Chem.* **1999**, *39*, 309.

(52) Dobkowski, J.; Herbich, J.; Galievsky, V.; Thummel, R. P.; Waluk, J. *Ber. Bunsen-Ges. Phys. Chem*. **1899**, *3*, 469.

(53) Herbich, J.; Dobkowski, J.; Thummel, R. P.; Hegde, V.; Waluk, J. *J. Phys. Chem. A* **1997**, *101*, 5839.

(54) Herbich, J.; Hung, C.-Y.; Thummel, R. P.; Waluk, J. *J. Am. Chem. Soc.* **1996**, *118*, 3508.

(55) Herbich, J.; Waluk, J.; Thummel, R. P.; Hung, C. Y. *J. Photochem. Photobiol. A: Chem.* **1994**, *80*, 157.

(56) Herbich, J.; Rettig, W.; Thummel, R. P.; Waluk, J. *Chem. Phys. Lett.* **1992**, *195*, 556.

(57) Del Valle, J. C.; Domínguez, E.; Kasha, M. *J. Phys. Chem. A* **1999**, *103*, 2467.

(58) Frisch, M. J.; Trucks, G. W.; Schlegel, H. B.; Scuseria, G. E.; Robb, M. A.; Cheeseman, J. R.; Zakrzewski, V. G.; Montgomery, J. A., Jr.; Stratmann, R. E.; Burant, J. C.; Dapprich, S.; Millam, J. M.; Daniels, A. D.; Kudin, K. N.; Strain, M. C.; Farkas, O.; Tomasi, J.; Barone, V.; Cossi, M.; Cammi, R.; Mennucci, B.; Pomelli, C.; Adamo, C.; Clifford, S.; Ochterski, J.; Petersson, G. A.; Ayala, P. Y.; Cui, Q.; Morokuma, K.; Malick, D. K.; Rabuck, A. D.; Raghavachari, K.; Foresman, J. B.; Cioslowski, J.; Ortiz, J. V.; Stefanov, B. B.; Liu, G.; Liashenko, A.; Piskorz, P.; Komaromi, I.; Gomperts, R.; Martin, R. L.; Fox, D. J.; Keith, T.; Al-Laham, M. A.; Peng, C. Y.; Nanayakkara, A.; Gonzalez, C.; Challacombe, M.; Gill, P. M. W.; Johnson, B.; Chen, W.; Wong, M. W.; Andres, J. L.; Gonzalez, C.; Head-Gordon, M.; Replogle, E. S.; Pople, J. A. *Gaussian 98, Revision A.6*; Gaussian, Inc.: Pittsburgh, PA, 1998.

(59) Schaftenaar, G. *Molden version 3.6*; CAOS/CAMM Center, Faculty of Science, University of Nijmegen, The Netherlands, **1991**.

(60) Scott, W. R. P.; Hünenberger, P. H.; Tironi, I. G.; Mark, A. E.; Billeter, S. R.; Fennen, J.; Torda, A. E.; Huber, T.; Krüger, P.; van Gunsteren, W. F. *J. Phys. Chem. A* **1999**, *103*, 3596.

(61) (a) van Gunsteren, W. F.; Billeter, S. R.; Eising, A. A.; Hunenberger, P. H.; Kruger, P.; Mark, A. E.; Scott, W. R. P.; Tironi, I. G. *Biomolecular Simulation: The GROMOS96 Manual and User Guide*; Biomos B. V.: Zürich, Groningen, 1996; (b) Duara, X.; Mark, A. E.; van Gunsteren, W. F. *J. Comput. Chem*. **1998**, *19*, 535.

(62) Jorgensen, W. L.; Modura, J. D.; Carol, J. S. *J. Am. Chem. Soc.* **1984**, *106*, 6638.

(63) Berendsen, H. J. C.; Pastma, J. P. M.; van Gunsteren, W. F.; Nola, A.; Haak, J. R. *J. Chem. Phys.* **1984**, *81*, 3684.

(64) Ryckaert, J. P.; Ciccott, G.; Berendsen, H. J. C. *J. Comput. Phys.* **1977**, *23*, 327.

(65) Laaksonen, L. *gOpenMol, version 1.21*; Centre for Scientific Computing, ESPOO, Finland, 1997.

(66) Łożyński, M.; Rusińska-Roszak, D.; Mack, H.-G. *J. Phys. Chem. A* **1998**, *102*, 2899.

(67) Sule, P.; Nagy, A. *J. Chem. Phys.* **1996**, *104*, 8524.

(68) Han, W.-G.; Suhai, S. *J. Phys. Chem*. **1996**, *100*, 3942.

(69) A Del Bene, J. E.; Person, W. B.; Szczepaniak, K. *J. Phys. Chem.* **1995**, *99*, 10705.

(70) Novoa, J. J.; Sosa, C. *J. Phys. Chem.* **1995**, *99*, 15837.

(71) Rablen, P. R.; Lockman, J. W.; Jorgensen, W. L. *J. Phys. Chem. A* **1998**, *102*, 3782.

(72) Fang, W. H. *J. Chem. Phys.* **1998,** *111* (12), 5361.